Characterization of Microwave Plasma Torch for Decontamination

Tetsuji Shimizu,* Bernd Steffes, René Pompl, Ferdinand Jamitzky, Wolfram Bunk, Katrin Ramrath, Matthias Georgi, Wilhelm Stolz, Hans-Ulrich Schmidt, Takuya Urayama, Shuitsu Fujii, Gregor Eugen Morfill

An atmospheric low-temperature microwave plasma torch has been developed and applied to disinfection. The size of the plasma output is relatively large (35 mm in diameter). Ar gas at a flow rate of 2.2 slm and 85 W microwave power are used. Plasma discharges are produced between the tip of each electrode and the inner surface of the cylinder. When an *Escherichia coli* culture is placed for 2 min at 20 mm below the torch, where the gas temperature is sufficiently cool, the bacteria are almost completely killed within a 40 mm diameter circle. The UV radiation is one of the major players responsible for killing bacteria, others being the reactive species and the charged particles.

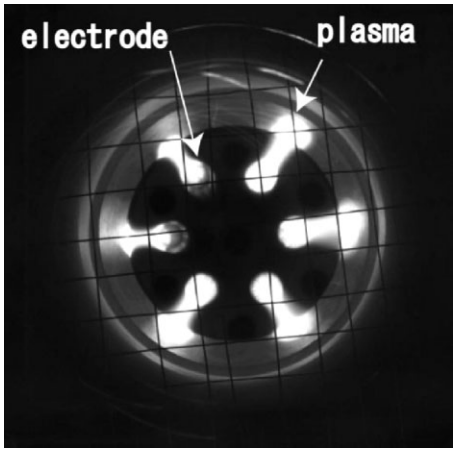

Introduction

Research in atmospheric plasma sources has been quite active, since these combine many advantages, such as low cost, simple design and easy handling.[1] Starting with the time when non-thermal atmospheric discharge sources became established, various medical applications have been investigated with growing interest. Even in a room-temperature plasma at atmospheric pressure, many chemical reactions are expected due to the presence of high energy electrons. These discharges can be utilized for the cleaning of medical equipment.[2,3] In addition, by using atmospheric plasmas, it is possible to treat substances which are not compatible with high vacuum, such as living organisms.[4–18] Contact-free treatments can be achieved without any heating and painful sensations.

In our group, a new atmospheric pressure plasma device (a microwave plasma torch) has been developed and tested in view of applying this new technique to the therapy of chronic foot and leg ulcers. In this article, basic device characteristics and measurements of plasma effects on bacteria cultures are discussed.

T. Shimizu, B. Steffes, R. Pompl, F. Jamitzky, W. Bunk, G. E. Morfill
Max-Planck Institute for Extraterrestrial Physics, Giessenbachstraße, D-85748 Garching, Germany
Fax: +49 89 3000 3510; E-mail: tshimizu@mpe.mpg.de
K. Ramrath, M. Georgi, W. Stolz
Clinic of Dermatology, Allergology and Environmental Medicine, Hospital Munich Schwabing, Kölner Platz 1, D 80804 München, Germany
H.-U. Schmidt
Institute for Medical Microbiology, Hospital Munich Schwabing, Kölner Platz 1, D 80804 München, Germany
T. Urayama, S. Fujii
ADTEC Plasma Technology Co. Ltd., Hikino-cho 5-6-10, 721-0942 Fukuyama, Japan

DOI: 10.1002/ppap.200800021

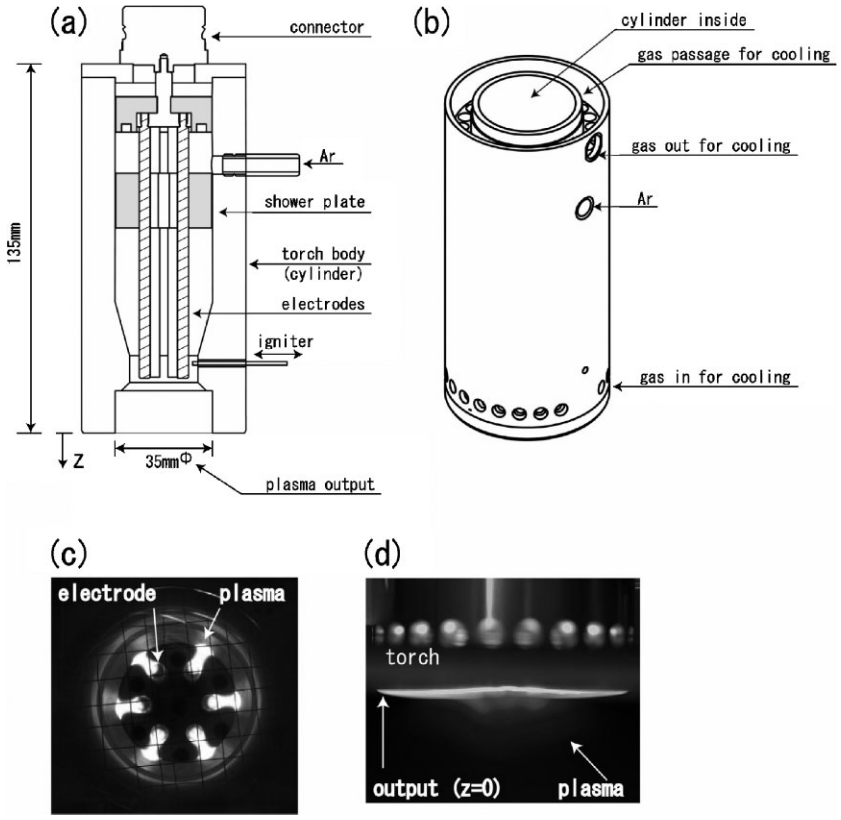

Figure 1. Schematic view of the plasma torch system and of the plasma: a) plasma torch, b) torch's cylinder, c) plasma between the electrodes and the cylinder, and d) plasma below the torch, view from the side.

Experimental Part

In Figure 1(a), a detailed view of the plasma torch is shown. The plasma torch consists of 6 stainless steel electrodes placed inside an aluminum cylinder which is 135 mm long. The centers of the 6 electrodes, whose surfaces are serrated, are equally distributed at a distance of 6 mm from the inner surface of the cylinder. The diameter of the electrodes and the distance between the electrodes and the surface of the cylinder are 4 mm. Through a series of different designs, it was found that this geometric configuration gave the most stable plasma yield for a given input power. The material and serrated structure of the electrodes are important for the triggering and stability of the discharge. The tips of the electrodes are situated at 20 mm from the opening of the torch. Since the typical size of chronic wounds is relatively large, our torch's opening is also relatively large (35 mm in diameter) in comparison with many other plasma devices used for medical purposes. Usually the torch is placed with the principal axis perpendicular to the ground. We examined the effect of tilting the torch and found that the torch could be used between $\pm 45^{\circ}$. In this study, only Ar gas (purity 99.998%) is used to produce the plasma in order to minimize the production of toxic products. Ar gas was flown at 2.2 slm from the base of the electrodes through a Teflon shower plate which regulates gas flow around the electrodes. Microwave power at 2.45 GHz is applied to the electrodes via a 2-stub tuner and coaxial cables which are 2 m long. The microwave power is set at 85 W. Six plasma zones are produced between each of the electrode's tips and the inner surface of the cylinder as shown in Figure 1(c). The torch is cooled by an air flow, which is produced inside the cylinder by a pump as shown in Figure 1(b). The maximum temperature of the torch surface is 320 K during the experiments. Figure 1(d) shows a side view of the plasma flow below the torch (the exposure time of the photo is 30 s). The shape of the plasma looks conical.

Both the gas temperature in the plasma flow below the torch, and the surface temperature of the agar plates were measured by a small thermocouples (type K). To obtain plasma profiles below the torch, a mesh grid electrode (20 lpi), which covers the whole opening of the torch, was used to measure the floating potential with respect to the ground. The voltmeter used had a 20 MΩ internal impedance. NO_2 concentration was measured by a gas detector (Dräger Multiwarn II).

To evaluate the electron density in the flow exiting the plasma torch, the resistance in a certain volume was measured. Two small Cu probes (3 mm in diameter) were placed at a distance which varies between 1.5 and 4 mm. Both probes were covered with Teflon tubes (5 mm in diameter), with the exception of the surfaces facing each other. A DC voltage of 0–18 V was applied between the probes. The electron density was estimated from measurements of the current I passing through the volume between the probes.

UV optical emission spectroscopy and UV power density measurement were carried out in order to assess the effect of ultraviolet radiation produced by the torch on bacteria. An optical fiber (HAMAMATSU A9762-01) connected to an optical spectrometer (HAMAMATSU TM-UV/VIS C10082CA) faced the plasma production region inside the plasma torch. The light emission from the plasma production region was much stronger than that from the other region. The distance between the plasma torch and the fiber surface was 5 cm. In addition, a z-profile (z: distance from the torch's opening) of the UV light radiation power density was measured by a power meter (HAMAMATSU UV Power Meter C8026) between 160 and 360 nm.

Escherichia coli (ATCC No. 9637) bacteria, inoculated on agar plates (88 mm in diameter), were used. The disinfection result was observed following a 16 h incubation of the culture at 308 K. The number density on the agar plate was found to be $\approx 0.5 \times 10^6$ cm^{-2} by using a dilution technique.

During the experiments, the ambient pressure was 950 ± 20 hPa, the temperature was 297 ± 2 K, and the relative humidity was $40 \pm 5\%$.

DOI: 10.1002/ppap.200800021

Results and Discussion

We investigated the axial profile of the gas temperature and the floating potential of the mesh grid electrode. The room temperature was 298 K. Figure 2 shows the *z*-profiles of the measured gas temperature, the NO_2 concentration along the torch axis, and the floating potential of the mesh grid electrode. In the vicinity of the torch, the gas temperature is relatively high (over 500 K). However, starting from $z = 5$ mm, the gas temperature has decreased drastically. As *z* increases further, the temperature decreases more gradually. At $z = 17$ mm, the temperature is 301 K, low enough for '*in vivo*' application.

The maximum NO_2 concentration (6.2 ppm) is observed at $z = 10$ mm. This is an indication that the plasma flow from the torch has developed a good contact with the ambient air around this position, which corresponds well with the temperature profile.

Inside the plasma torch, there is relatively strong light emission between the electrodes and the cylinder. However, the intensity of the light coming from the plasma flow exiting the torch is weak, especially below $z = 15$ mm. In order to determine how the plasma is distributed below the torch, the floating potential of the mesh grid electrode is measured. The potential also decreases as *z* increases, almost in the same way as the gas temperature as shown in Figure 2. Around $z = 20$ mm, the measured potential is not 0. This indicates that there are charged particles.

We observed the plasma exposure effect on bacteria. For example, when an *E. coli* culture is placed 20 mm away from the output of the torch for 2 min, a clearly visible bactericidal effect can be found. This is observable as a zone of inhibition of growth on the agar plate as shown in Figure 3, indicating that the bacteria within a circle of 40 mm diameter have been killed. The boundary of the zone of inhibition is a little fuzzy, and the zone of inhibition is slightly larger than the opening of the torch. We measured the surface temperature of the agar plate during the treatment. Within 2 min of treatment, the temperature increased by 4.5° and reached 300 K. Thus, the heat effect can be ruled out for killing bacteria in our experiments. As a control, the impact of the Ar gas flow on bacteria is examined, and the *E. coli* culture is treated without plasma for 10 min. The other experimental conditions are the same as in the experiment presented in Figure 3. After 16 h of incubation, a homogeneous growth of bacteria is observed on the treated area. Thus, there is no effect caused by the Ar gas flow in respect with killing bacteria using our device.

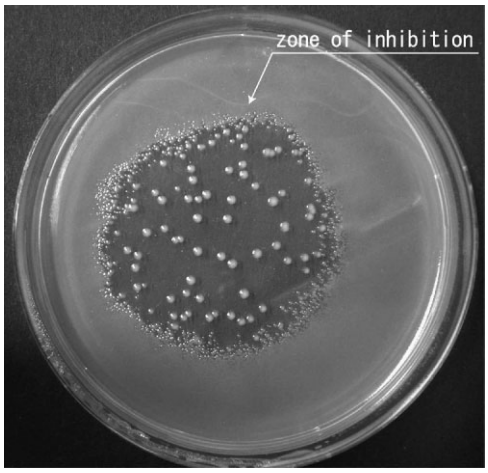

Figure 3. E. coli culture on an agar plate after plasma treatment for 2 min. The culture is placed at $z = 20$ mm, and the image was taken after 16 h incubation.

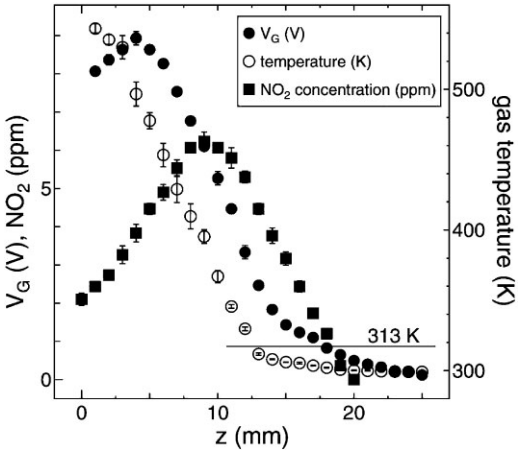

Figure 2. Gas temperature, NO_2 concentration and floating potential as a function of the distance *z* from the torch.

The current *I* which flowed in the volume between the two probes is shown in Figure 4. In this experiment, the distance between the probes is 1.5 mm and the applied voltage is 0 or 9.4 V. When no voltage (0 V) is applied, there is almost no current. When 9.4 V is applied between the probes, *I* is 3.2 nA in the vicinity of the torch. *I* decreases with increasing *z* almost similarly with the variation of the floating potential presented in Figure 2. The electrical resistance *R* between the probes can be treated as a pure resistance, since *I* increases linearly when the voltage between the probes is varied between 0 and 18 V, and varies inversely proportional with the distance between the probes in the range from 1.5 to 4 mm.

In order to evaluate the electron density, we make the following assumptions: The current flows only in the column formed by the area of the probes and the length between the two probes. Moreover, the collisions between neutrals and electrons are considered to be elastic. The Ar

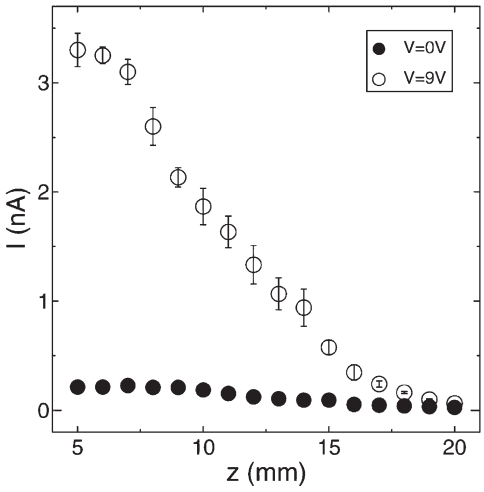

Figure 4. Current *I* between 2 probes as a function of *z*. The applied voltage between the probes is 0 and 9 V.

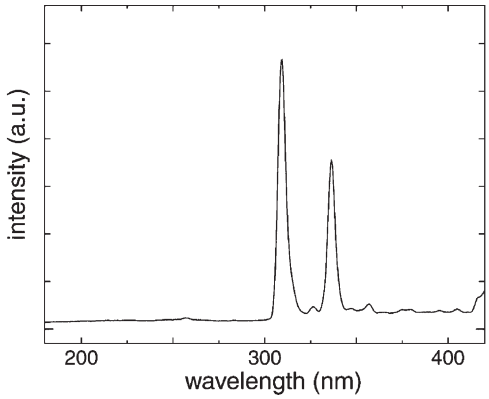

Figure 5. Optical emission spectrum from the torch in the UV region. There are two strong peaks in UV-B region.

atoms in the column are present only as neutrals. In this case, the electrical conductivity σ is written as $\sigma = e^2 n / m\nu_{en}$, where n, m, are ν_{en} are the electron density in the measured column, the electron mass, and the collision frequency between electrons and neutrals, respectively. R is given by $R = (1/\sigma)\,(d/S)$, where d and S are the distance between the electrodes and the area of the electrodes, respectively. Considering the equilibrium between the Coulomb force and the friction force for the case of electrons, we obtain $\nu_{en} = eE/mv$. Here, E is the electric field between the electrodes, and v is the drift velocity of electrons. An expression for v is given in ref.[19], assuming that E is constant in the measured volume, When we consider the applied voltage of 9.4 V between the electrodes separated by a distance of 1.5 mm, we obtain $v = 3 \times 10^3$ m $\cdot$ s^{-1}. At $z = 20$ mm, the current is 0.06 nA. Using the equations above, the electron density is determined to be $n = 1.8 \times 10^4$ cm^{-3}. This indicates that bacteria at this position can acquire an electrical charge.

An example of the UV radiation spectrum obtained from the plasma torch is shown in Figure 5. There are two strong peaks in the UV-B region, and there is no strong line in the UV-C region. Figure 6 shows a *z*-profile of the integrated UV power density. The sensor is placed at the center axis of the plasma torch. The UV power density decreases monotonically as *z* increases. This means that the main light source is only the plasma production region in the plasma torch. At the position where the samples are placed ($z = 20$ mm), the UV power is 80 μW $\cdot$ cm^{-2}

In order to determine the effect of the UV radiation on bacteria, a quartz glass is placed between the plasma torch and the samples. The quartz glass is 10 mm thick and larger than the agar plates (95 mm in diameter). When the quartz glass is placed between the sensor and the plasma torch, the UV power density decreased to 60 μW $\cdot$ cm^{-2} at $z = 20$ mm.

Figure 7 shows results of the plasma treatment on bacteria with and without the quartz glass. Figure 7 a) and b) show the bactericidal effects on the samples after 2 and 4 min treatments, respectively. When the samples are treated without the quartz glass, the size of the inhibition zone increases with increasing the treatment time. When the quartz glass is placed between the torch and the samples, the results are shown in Figure 7 c) and d) for 2 and 4 min treatments, respectively. Since the quartz glass fully covers and seals the samples, only the UV radiation can penetrate to reach the surfaces of the samples. When the sample is treated with the quartz glass cover for 4 min, the bactericidal effect shown in Figure 7 d) is observed. The zone of inhibition is smaller than that of the corresponding treatment without the quartz glass.

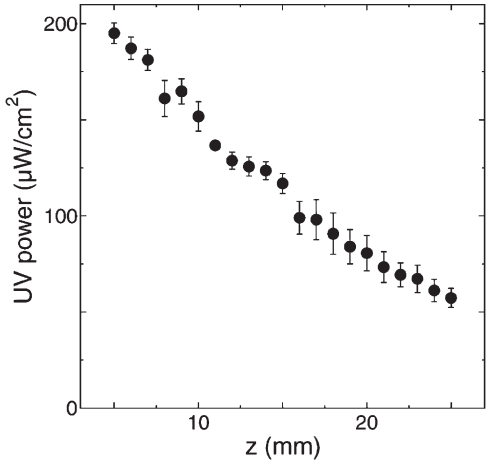

Figure 6. UV power density measurements as a function of *z*.

DOI: 10.1002/ppap.200800021

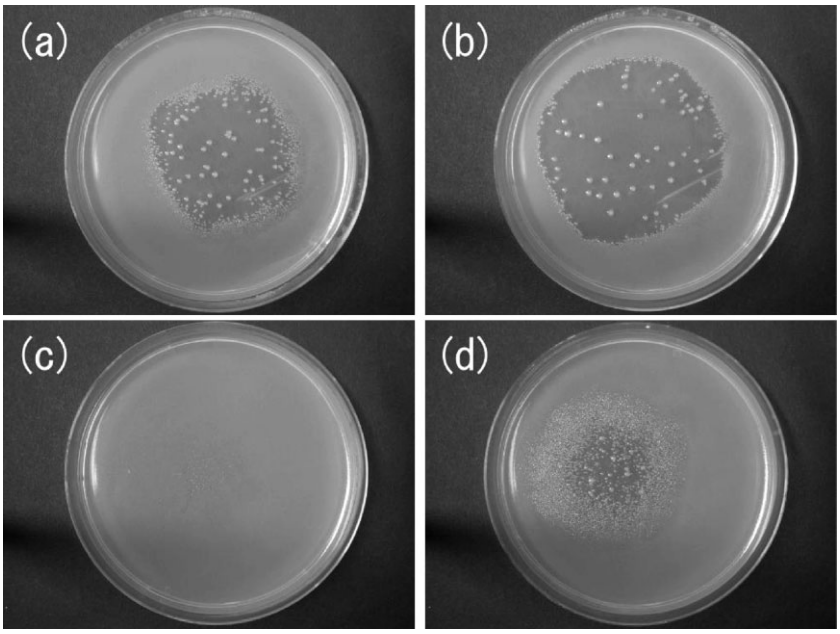

Figure 7. Bactericidal effects on *E. Coli* cultures with different conditions. a) 2 min treatment without quartz glass between torch and sample, b) 4 min treatment without quartz glass, c) 2 min-treatment with quartz glass, d) 4 min treatment with quartz glass.

The results are summarized in Figure 8, where the diameters of the inhibition zones are plotted from 5 experiments. From these results, we can conclude that that UV light is one important agent for killing bacteria in our experiments, however there are other mechanisms, e.g. charged particles[20,21] in the plasma and reactive species[4,21] which are produced during the interaction of plasma with ambient air.

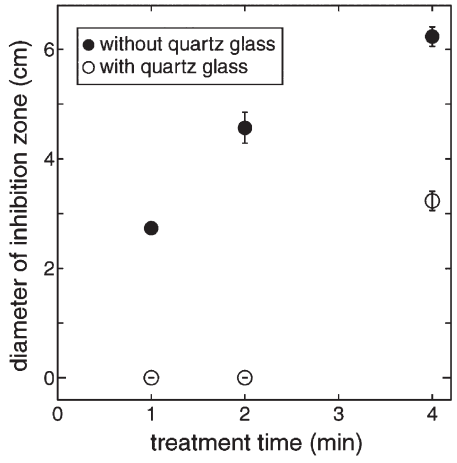

Figure 8. Diameter of the inhibition zone as a function of treatment time. The experiments were carried out with and without quartz glass.

Conclusion

In conclusion, a large area microwave plasma torch has been developed for the purpose of "*in vivo*" bacterial disinfection. By using 2.2 slm of Ar gas flow and 85 W of microwave power at atmospheric pressure, we obtained plasmas with characteristics which are suitable for medical applications and treatment. Tests with cultures of *E. coli* (and others) have proven the bactericidal effect. UV radiation was found to be one major agent responsible for killing bacteria, however there are other mechanisms involved in sterilization of bacteria cultures. We consider that this technique can be used for a number of different medical applications, in particular wound healing, and have started a clinical study for the therapy of chronic foot and leg ulcers.

Received: January 31, 2008; Revised: March 16, 2008; Accepted: March 31, 2008; DOI: 10.1002/ppap.200800021

Keywords: microwave discharges; non-thermal plasmas; plasma treatment; therapy of chronic foot ulcers

[1] J. Park, I. Henins, H. W. Hermann, G. S. Selwyn, R. F. Hicks, *J. Appl. Phys.* **2001**, *89*, 20.
[2] J. G. Birmmingham, D. J. Hammerstrom, *IEEE Trans. Plasma Sci.* **2000**, *28*, 51.
[3] M. Laroussi, *IEEE Trans. Plasma Sci.* **2002**, *30*, 1409.
[4] T. C. Montie, K. Kelly-Wintenberg, J. R. Roth, *IEEE Trans. Plasma Sci.* **2000**, *28*, 41.
[5] K. Kelly-Wintenburg, D. M. Sherman, P. P.-Y. Tsai, R. B. Gardi, F. Karakaya, Z. Chen, J. R. Roth, T. C. Montie, *IEEE Trans. Plasma Sci.* **2000**, *28*, 64.
[6] E. Stoffels, A. J. Flikweert, W. W. Stoffels, G. M. W. Kroesen, *Plasma Sources Sci. Technol.* **2002**, *11*, 383.
[7] G. Fridman, A. Shereshevsky, M. M. Jost, A. D. Brooks, A. Fridman, A. Gutsol, V. Vasilets, G. Friedman, *Plasma Chem. Plasma Process.* **2007**, *27*, 163.
[8] G. Fridman, A. D. Brooks, M. Balasubramanian, A. Fridman, A. Gutsol, V. N. Vasilets, H. Ayan, G. Friedman, *Plasma Process. Polym.* **2007**, *4*, 370.
[9] R. E. J. Sladek, E. Stoffels, R. Walraven, P. J. A. Tielbeek, R. A. Koolhoven, *IEEE Trans. Plasma Sci.* **2004**, *32*, 1540.
[10] M. Moisan, J. Barbeau, S. Moreau, J. Pelletier, M. Tabrizian, L. H. Yahia, *Int. J. Pharm.* **2002**, *226*, 1.
[11] B. J. Park, D. H. Lee, J.-C. Parka, I.-S. Lee, K.-Y. Lee, S. O. Hyun, M.-S. Chun, K.-H. Chung, *Phys. Plasmas* **2003**, *10*, 4539.
[12] T. Akitsu, H. Ohkawa, M. Tsuji, H. Kimura, M. Kogoma, *Surf. Coat. Technol.* **2005**, *193*, 29.

[13] M. Laroussi, X. Lu, *Appl. Phys. Lett.* **2005**, *87*, 113902.
[14] J. Goree, B. Liu, D. Drake, E. Stoffels, *IEEE Trans. Plasma Sci.* **2006**, *34*, 1317.
[15] T. Sato, T. Miyahara, A. Doi, S. Ochiai, T. Urayama, T. Nakatani, *Appl. Phys. Lett.* **2006**, *89*, 073902.
[16] X. T. Deng, J. J. Shi, G. Shama, M. G. Kong, *Appl. Phys. Lett.* **2006**, *87*, 153901.
[17] Q. S. Yu, C. Huang, F.-H. Hsieh, H. Huff, Y. Duah, *Appl. Phys. Lett.* **2006**, *88*, 013903.
[18] E. Stoffels, *Contrib. Plasma Phys.* **2007**, *1-2*, 40.
[19] N. E. Levine, M. A. Uman, *J. Appl. Phys.* **1964**, *35*, 2618.
[20] D. A. Mendis, M. Rosenberg, F. Azam, *IEEE Trans. Plasma Sci.* **2000**, *28*, 1304.
[21] M. Laroussi, D. A. Mendis, M. Rosenberg, *New J. Phys.* **2003**, *5*, 41.

DOI: 10.1002/ppap.200800021